INTERNATIONAL JOURNAL FOR NUMERICAL METHODS IN FLUIDS
Int. J. Numer. Meth. Fluids 2008; **56**:1583–1588
Published online 19 September 2007 in Wiley InterScience (www.interscience.wiley.com). DOI: 10.1002/fld.1612

A reduced model of the Madden–Julian oscillation

Nils P. Wedi[1,*,†] and Piotr K. Smolarkiewicz[2]

[1]*European Centre for Medium Range Weather Forecasts, Shinfield Park, Reading RG2 9AX, U.K.*
[2]*National Centre for Atmospheric Research, Boulder, CO 80307, U.S.A.*

SUMMARY

We have extended our virtual laboratory for internal wave motions (*Int. J. Numer. Meth. Fluids* 2005; **47**:1369–1374) to the case of rotating fluids on an equatorial β-plane. A virtual wave-maker is introduced *via* a time-dependent coordinate transformation in the meridional direction, represented by two lateral boundary meanders. The technique is consistently incorporated into the numerical algorithm of the nonhydrostatic model EULAG. The modelling framework is applied in simulations of equatorial wave motions to enhance our understanding of the Madden–Julian oscillation (MJO). The simulation of a realistic MJO in global circulation and climate models is a continuing challenge—in part, due to the failure of existing theories to explain the ubiquitous modelling difficulties of the phenomenon. Virtual laboratory experiments appear ideal complementary tools to isolate and study particular geophysical flow structures. In these laboratory-scale 'climate' simulations we observe eastward propagating low-frequency horizontal structures consistent with Rossby solitary wave theory, representing a particular solution of the Korteweg–de Vries equation for the evolution of the wave amplitude under a given forcing. The latter extends the linear shallow water theory—commonly used to explain different modes of equatorial wave motions—to the weakly nonlinear regime. One important outcome of our simulations is the finding that these structures depend on strong stratification, and may be easily destroyed or weakened if substantial near-surface perturbations and associated vertical motions exist. This could play a role in the failure to simulate a realistic MJO, but it may also provide an explanation why solitary waves are not as readily observed in oceans as they are in models and theory. Ultimately, our research aims at constructing a simplified dynamical apparatus to reproduce MJO-like structures in a laboratory analogue, in the spirit of the Plumb–McEwan experiment for the quasi-biennial oscillation and *vis-a-vis* its numerical equivalent.

Received 30 March 2007; Revised 26 July 2007; Accepted 30 July 2007

KEY WORDS: MJO; Korteweg–de Vries equation; solitary wave; generalized coordinate transformation; equatorial β-plane; tank experiment; EULAG

*Correspondence to: Nils P. Wedi, European Centre for Medium Range Weather Forecasts, Shinfield Park, Reading RG2 9AX, U.K.
†E-mail: wedi@ecmwf.int

1. INTRODUCTION

The Madden–Julian oscillation (MJO) [1] is the main intraseasonal atmospheric fluctuation in the equatorial troposphere affecting weather in large parts of the world. Polynesian seamen are believed to have used the phenomenon to sail eastward in the trade wind-dominated equatorial Pacific 4500 years ago [2]. Despite substantial efforts a reliable forecasting of the MJO and understanding its mechanisms remain key challenges in atmospheric science. Diabatic processes associated with tropical convection and two-way atmosphere–ocean interaction are generally believed to be crucial in explaining the MJO. A number of theories have been put forward to explain the life cycle of MJO events, which has been comprehensively reviewed in [2]. Incorporating elements from various theories, we synthesize the importance of the interaction and feedback processes of convection, large-scale dynamics, and surface fluxes. The complexity of the processes involved—due to their multi-scale nature [3] ranging from micro to global scales—render the MJO an intriguing problem in fluid dynamics, not least because of its appearance as a solitary structure and the inherent difficulty to model it with state-of-the-art global numerical weather prediction and climate models.

Based on the experience [4, 5] in modelling the laboratory analogue of the quasi-biennial oscillation [6]—an equally intriguing wave-driven equatorial phenomenon—we explore the possibility of a virtual laboratory experiment for the MJO. To further the understanding of the principal mechanism underlying the MJO dynamics we conduct a series of large-eddy simulations of rotational flows on a zonally periodic equatorial β-plane, using the Eulerian/semi-Lagrangian, nonoscillatory, forward-in-time (NFT), nonhydrostatic model EULAG; see [7] and references therein. External heating is imposed (optionally) at the bottom and/or at the meridional boundaries of the domain. In particular, we explore sensitivities of numerical solutions to variations in meridionally undulating lateral boundaries that induce Rossby waves, mean shear, and time variability of the zonal-mean zonal flow. The undulating boundaries are incorporated into the numerical algorithm *via* time-dependent coordinate transformations in the meridional direction [7, 8]. Such undulations can generate long-lived horizontal structures [9], which resemble a robust low-wavenumber and low-frequency signature in the observed wave spectra, reminiscent of the MJO. We test the hypothesis that for long time- and length scales MJO-like structures may propagate eastward as a result of weakly nonlinear externally forced wave dynamics. There have been earlier attempts to investigate the role of nonlinearity for low-frequency equatorial waves [10, 11], but their findings were either negative or inconclusive. More recently, there have been attempts to explore the weakly nonlinear regime based on the forced Korteweg–de Vries equation [12], which may be rigorously derived from the quasi two-dimensional system described in the next section. Rossby solitary waves represent a special solution of this system given the right balance between nonlinearity and Rossby wave dispersion [13]. These solitary structures may propagate eastward under certain circumstances. What makes this theory particularly attractive is that it extends the linear shallow water theory—commonly used to explain different modes of equatorial wave motions—to the weakly nonlinear regime. Notably, most or all spectral signals of convectively coupled equatorial waves can be explained *via* the linear theory [14], except one of the most dominant low-frequency spectral peaks, that is the MJO *per se*.

2. THE NUMERICAL MODEL

The numerical model set-up is similar to the set-up in [5], notably with an advantage compared with actual laboratory experiments, in which the emulation of equatorial dynamics and the beta effect

DOI: 10.1002/fld

in particular is difficult [15]. The equations of motion for a rotating, density-stratified Boussinesq fluid are

$$\nabla\cdot(\rho_0\mathbf{v})=0$$

$$\frac{\mathrm{D}\mathbf{v}}{\mathrm{D}t}=-\nabla\pi'+\mathbf{g}\frac{\rho'}{\rho_0}-\mathbf{f}\times\mathbf{v}'+\mathbf{F}_\mathbf{v} \tag{1}$$

$$\frac{\mathrm{D}\rho'}{\mathrm{D}t}=-\mathbf{v}\cdot\nabla\rho_e+F_\rho$$

Here, the operators $\mathrm{D}/\mathrm{D}t$, ∇, and $\nabla\cdot$ symbolize the material derivative, gradient, and divergence; $\mathbf{v}$ denotes the velocity vector; $\mathbf{v}'$, ρ', and π' denote, respectively, velocity, density and normalized-pressure perturbations with respect to a prescribed balanced ambient state with geostrophic wind $\mathbf{v}_e$ and linearly stratified ρ_e profile; $\mathbf{f}$ and $\mathbf{g}$ symbolize the vectors of the 'Coriolis parameter' and gravity (both vertically oriented), where $\|\mathbf{f}\|=f_0+\beta y$ with f_0 and β constant; ρ_0 denotes a uniform reference density. Frictional terms at $q=y,z$-boundaries are of the form $F_\rho(q):=\tau_\rho^{-1}\mathrm{e}^{-q/h}(\rho-\rho_b)$ and $\mathbf{F}_\mathbf{v}(q):=\tau_\mathbf{v}^{-1}\mathrm{e}^{-q/h}(\mathbf{v}-\mathbf{v}_b)$, with subscript b denoting a prescribed boundary value; time scales are $\tau_\rho=\Delta z^2/\kappa$ and $\tau_\mathbf{v}=0.125\tau_\rho$ (assuming diffusion of heat in water, $\kappa=1.39\times10^{-7}\,\mathrm{m}^2\,\mathrm{s}^{-1}$) and height scale $h=2\Delta z$, where Δz is the vertical gridsize. Given the model's formulation in density, heating is included indirectly *via* the gradient of density at the lower boundary, which induces convective vertical motions of Rayleigh–Bénard type. The frictional boundary layer is emulated by the term $\mathbf{F}_\mathbf{v}$ in the momentum equation in (1).

Equations (1) are cast in a time-dependent curvilinear framework [7, 8], employing the similarity transformation

$$\overline{t}=t,\quad \overline{x}=x,\quad \overline{y}=y_0\frac{y-y_S(x,y,t)}{y_N(x,y,t)-y_S(x,y,t)},\quad \overline{z}=z \tag{2}$$

Unless stated otherwise, the meridional boundaries of the equatorial β-plane simulations are given as

$$y_S(x,y,t)=0.5\varepsilon(\sin(k_x x-\omega_1 t)+\sin(k_x x-\omega_2 t)) \tag{3}$$

and $y_N(x,y,t)=y_0-y_S(x,y,t)$, with domain size $x_0=4.3\,\mathrm{m}$ and $y_0=4\,\mathrm{m}$, amplitude $\varepsilon=0.2$, $k_x=2\pi s/x_0$ with mode $s=6$, and forcing frequencies $\omega_1=2\pi/120\,\mathrm{s}^{-1}$, and $\omega_2=2\pi/100\,\mathrm{s}^{-1}$, respectively. Transformation (2) allows for time-dependent boundary forcings, $y_N(x,y,t)$ and $y_S(x,y,t)$, free of small-amplitude approximations. It describes a translating and pulsating meander (a similar forcing is provided in case (d) of [9]) and may be understood as a sophisticated wave-maker for virtual laboratory experiments.

The governing equations (1) are integrated numerically in the transformed space using a second-order-accurate, semi-implicit, flux-form Eulerian NFT approach, broadly documented in the literature, cf. [16]. The numerical algorithm is based on the monotone MPDATA transport scheme [17]. For the adiabatic dynamics all prognostic equations in (1) are integrated using the trapezoidal rule, treating all forcings on the rhs implicitly; frictional and heating terms are computed explicitly, to the first-order. Together with the curvilinearity of the coordinates, this leads to a complicated elliptic problem for pressure (see Appendix A in [7] for the complete description) solved iteratively using the preconditioned generalized conjugate-residual approach—a nonsymmetric Krylov-subspace solver [18].

DOI: 10.1002/fld

3. THE MADDEN–JULIAN OSCILLATION ANALOGUE

The model's ability to simulate free topographic Rossby modes in a laboratory set-up is tested against the analytical solution for the first Rossby normal mode in a closed rectangular β-plane without lateral forcing (see [19] for a description). The model set-up represents a quasi-two-dimensional simulation. In this case, the model is run in the computational domain $4.3\times2.0\times0.45\,\mathrm{m}$, with $128\times128\times3$ gridpoints. Utilizing the dynamical equivalence of the β-plane approximation and the variation of topography in a laboratory, the model parameters are set as follows: $f_0\equiv2\omega$ and $\beta\equiv2\omega s_y/H_0$; with angular velocity $\omega=2\pi/T_0$, the rotating turntable period $T_0=45\,\mathrm{s}$, slope $s_y=0.15$, and mean depth $H_0=0.45\,\mathrm{m}$. The model is set for frictionless flow with an unstratified, stagnant ambient state, and is initialized with the analytic solution for a rectangular basin (cf. [20, p. 147]). The accuracy is measured by comparing the time series of the meridional velocity component for selected points at mid-channel of the domain with the analytical oscillation period of the lowest eigenperiod, cf. [19, 20]. We obtain an average oscillation period of 4.0 min compared with the analytic solution of 3.9 min. Note, that there can be considerable departures in real laboratory experiments (see [19] for a discussion).

We modify the testing set-up above by setting a zonally periodic, equatorial β-plane ($f_0=0$, $\beta=2\omega/a$, $a=3\,\mathrm{m}$), by doubling the domain in the meridional direction ($y_0=4\,\mathrm{m}$), and by adding the lateral forcing described in Equations (2) and (3) together with a zonal background flow $u_e=0.05\,\mathrm{m}$. The upper and lower boundaries are rigid while the lateral meridional boundaries are impermeable. With such a set-up, the numerical model mimics the forced nonlinear, rigid-lid shallow water equations on a β-plane—an archtype for equatorial wave motions.

The model is run for upto 8 h (timestep $\mathrm{d}t=0.1\,\mathrm{s}$), which essentially represents a laboratory-scale 'climate' simulation. The principal result is that the lateral undulations, as given in Equations (2) and (3), generate long-lived horizontal structures (cf. [9]) that resemble a robust low-wavenumber and low-frequency signature in observed wave spectra. We have performed a series of simulations exploring the parametric sensitivities. Both the specified lateral forcing and the Coriolis force are found to be the important elements for attaining long-lived, large-scale coherent structures in the quasi-two-dimensional set-up. With different forcings on each side of the domain or random forcings (i.e. altering y_S and y_N in Equation (2) independently), or only a single frequency forcing, we do not normally find a dominant low-frequency spectral signal. In contrast, when the oscillatory boundary forcing is applied only on one side of the domain in a hemispheric β-plane (one boundary represents the equator) we also obtain an eastward propagating wavenumber-one structure.

In three dimensions, our virtual laboratory tank is represented by a zonally periodic, rectangular computational domain consisting of $128\times128\times64$ grid points, where we reduce the height to $H_0=0.11\,\mathrm{m}$, to enhance the vertical resolution (while keeping β as before). Furthermore, we introduce a bottom boundary layer heating and friction as described in Section 2.

Interestingly, we have been unable to show the existence of the same low-wavenumber and low-frequency signature in the unstratified three-dimensional simulations, as we have found in the quasi two-dimensional cases. Instead we observe a broad range of westward propagating signals (not shown), unless the meridional extent of the domain is decreased to $y_0=1.5\,\mathrm{m}$ or below, in which case the beat frequency $\omega_2-\omega_1$ of the boundary forcing dominates. However, this changes dramatically if we introduce strong vertical stratification $\rho_e=\rho_0(1-\mathscr{S}z)$, with $\mathscr{S}=N^2/g$, gravity $g=9.8065\,\mathrm{m\,s^{-2}}$, and a Brunt–Väisällä frequency $N=1.566\,\mathrm{s^{-1}}$. Now we obtain a significant eastward propagating wavenumber-one signal with periods of around 1 h. Figure 1 shows the Hovmoeller diagram of velocity potential anomaly at the height 0.75 H_0. The data has been

DOI: 10.1002/fld

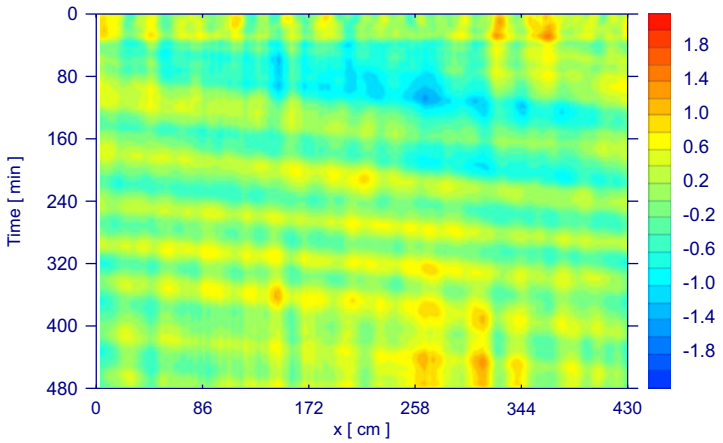

Figure 1. Hovmoeller diagram of velocity potential anomaly ($\times 10^{-3}\,\mathrm{m^2\,s^{-1}}$) at the height 0.75 H_0 of the stratified three-dimensional simulation.

averaged over the near-equatorial region ± 0.78125 m from the mid-channel and low-pass filtered to remove the beat frequency of the boundary oscillation. Notably, we allow convection to develop freely in the first 33 min of the simulation, before starting to oscillate the lateral boundaries. The initial period can be clearly seen as a regime change in Figure 1 with the onset of zero or negative velocity potential.

In a series of three-dimensional simulations we have established that an increased magnitude of the imposed boundary layer heating can weaken or destroy the formation of the eastward propagating wavenumber-one signal (not shown). We also find that the principal result is independent of whether the bottom heating is applied uniformly or is zonally asymmetric, cf. [2]. Interestingly, we also observe a dominant zonal mean zonal flow oscillation (super-rotation) in our three-dimensional experiments with the same period as identified in the wavenumber-one spectral signal.

4. CONCLUSIONS

The virtual laboratory setup allows one to explore a number of otherwise difficult nonlinear flow phenomena. Despite its simplifications with respect to natural atmospheric processes, our β-plane model incorporates convective motions, externally driven large-scale dynamics and surface boundary layer fluxes due to imposed heating. We identify a number of wave motions in our simulations.

The principal result is that we obtain long-lived coherent structures as a result of lateral boundary meanders—as specified in Equations (2) and (3)—in both the quasi-two-dimensional and the three-dimensional simulations. Our quasi-two-dimensional results are consistent with the findings in [9] and may be explained analytically using weakly nonlinear theory of Rossby solitary waves (cf. references in [13]). We confirm that the results are applicable to three-dimensional baroclinic (equatorial) motions under the constraint of strong stratification $N \gg f$ (cf. [21, p. 449]). Our simulations further indicate that strong near-surface perturbations and resulting vertical motions can destroy the formation of such long-lived structures. These findings may be a step towards

DOI: 10.1002/fld

solving 'the mystery of the missing equatorial solitons' [13], where Rossby solitary waves are readily observed in models and theory but not in the ocean. Hence, for both numerical simulations and observations our study provides important sensitivities with respect to the dependence and the destruction of large-scale coherent structures in a three-dimensional, nonlinear flow. Finally, we conclude that our β-plane model exhibits significant similarities to the MJO of the tropical troposphere and these will be discussed thoroughly in a forthcoming publication.

REFERENCES

1. Madden RA, Julian PR. Detection of a 40–50 day oscillation in the zonal wind in the tropical Pacific. *Journal of Atmospheric Sciences* 1971; **28**:702–708.
2. Zhang C. Madden–Julian oscillation. *Reviews of Geophysics* 2005; **43**:1–36. DOI:10.1029/2004RG000158.
3. Biello J, Majda AJ. A new multiscale model for the Madden–Julian oscillation. *Journal of Atmospheric Sciences* 2005; **62**:1694–1721.
4. Wedi NP, Smolarkiewicz PK. Laboratory for internal gravity-wave dynamics: the numerical equivalent to the quasi-biennial oscillation (QBO) analogue. *International Journal of Numerical Methods in Fluids* 2005; **47**: 1369–1374.
5. Wedi NP, Smolarkiewicz PK. Direct numerical simulation of the Plumb–McEwan laboratory analog of the QBO. *Journal of Atmospheric Sciences* 2006; **63**(12):3226–3252.
6. Plumb RA, McEwan D. The instability of a forced standing wave in a viscous stratified fluid: a laboratory analogue of the quasi-biennial oscillation. *Journal of Atmospheric Sciences* 1978; **35**:1827–1839.
7. Prusa JM, Smolarkiewicz PK. An all-scale anelastic model for geophysical flows: dynamic grid deformation. *Journal of Computational Physics* 2003; **190**:601–622.
8. Wedi NP, Smolarkiewicz PK. Extending Gal-Chen & Somerville terrain-following coordinate transformation on time-dependent curvilinear boundaries. *Journal of Computational Physics* 2004; **193**:1–20.
9. Malanotte-Rizzoli PM, Young RE, Haidvogel DB. Numerical simulation of transient boundary-forced radiation. Part II: the Modon regime. *Journal of Physical Oceanography* 1988; **18**:1546–1569.
10. Van Tuyl AH. Nonlinearities in low-frequency equatorial waves. *Journal of Atmospheric Sciences* 1987; **44**: 2478–2492.
11. Zou J, Cho H-R. A nonlinear Schroedinger equation model of the intraseasonal oscillation. *Journal of Atmospheric Sciences* 2000; **57**:2435–2444.
12. Hodyss D, Nathan TR. Solitary Rossby waves in zonally varying jet flows. *Geophysical and Astrophysical Fluid Dynamics* 2002; **96**(3):239–262.
13. Boyd J. Equatorial solitary waves. Part V: initial value experiments, coexisting branches, and tilted-pair instability. *Journal of Physical Oceanography* 2002; **32**:2589–2602.
14. Wheeler M, Kiladis GN. Convectively coupled equatorial waves: analysis of clouds and temperature in the wave number-frequency domain. *Journal of Atmospheric Sciences* 1999; **56**:374–399.
15. Ohlsen DR, Rhines PB. Laboratory studies of equatorially trapped waves using ferrofluid. *Journal of Fluid Mechanics* 1997; **338**:35–58.
16. Smolarkiewicz PK, Prusa JM. Towards mesh adaptivity for geophysical turbulence: continuous mapping approach. *International Journal of Numerical Methods in Fluids* 2005; **47**:789–801.
17. Smolarkiewicz PK. Multidimensional positive definite advection transport algorithm: an overview. *International Journal of Numerical Methods in Fluids* 2006; **50**:1123–1144.
18. Smolarkiewicz PK, Margolin LG. Variational methods for elliptic problems in fluid models. *Proceedings of the ECMWF Workshop on Developments in Numerical Methods for Very High Resolution Global Models*. European Centre for Medium-Range Weather Forecasts: Reading, U.K., 2000; 137–159.
19. Pierini S, Fincham AM, Renouard D, D'Ambrosio MR, Didelle H. Laboratory modeling of topographic Rossby normal modes. *Dynamics of Atmospheres and Ocean* 2002; **35**:205–225.
20. Pedlosky J. *Geophysical Fluid Dynamics* (2nd edn). Springer: New York, 1987.
21. Gill A. *Atmosphere–Ocean Dynamics*. International Geophysics Series, vol. 30. Academic Press: London, 1982.

DOI: 10.1002/fld